

See discussions, stats, and author profiles for this publication at: <https://www.researchgate.net/publication/8346063>

# Nuclear Quantum Effects and Hydrogen Bonding in Liquids

ARTICLE *in* JOURNAL OF THE AMERICAN CHEMICAL SOCIETY · AUGUST 2003

Impact Factor: 12.11 · DOI: 10.1021/ja0351995 · Source: PubMed

---

CITATIONS

38

---

READS

19

2 AUTHORS, INCLUDING:



Simone Raugei

Pacific Northwest National Laboratory

96 PUBLICATIONS 1,722 CITATIONS

SEE PROFILE

## Nuclear Quantum Effects and Hydrogen Bonding in Liquids

Simone Rauegi<sup>\*,†</sup> and Michael L. Klein<sup>‡</sup>*International School for Advanced Studies, via Beirut 4, 34014 Trieste, Italy, and Center for Molecular Modeling and Department of Chemistry, University of Pennsylvania, Philadelphia, Pennsylvania 19104-6323*

Received March 18, 2003; E-mail: rauegi@sissa.it

Hydrogen bonding is one of the fundamental interactions in chemistry and biology. The structures of water and DNA are but two examples of the profound influence of the H-bond in determining the structure of matter. In addition to structure, H-bonds are also actively involved in chemical reactivity.<sup>1</sup> Despite the likely importance of zero point energy effects involving hydrogen, their explicit role in determining the structure of even simple H-bonded liquids has yet to be fully rationalized. Accordingly, herein, we analyze the influence of nuclear quantum (zero point energy) effects on the H-bonding in liquid hydrogen fluoride (HF) around its boiling point.<sup>2</sup>

HF is the simplest and one of the strongest known H-bonded systems. It, therefore, represents an important prototype for probing hydrogen bonding. H-bonds determine the structure of HF in all phases. For example, solid<sup>3</sup> and, to a lesser extent, liquid HF<sup>4,5</sup> consist of zigzag H-bonded chains, whereas the vapor phase is characterized by oligomers and cyclic clusters.<sup>6</sup>

Liquid HF has been investigated extensively using a variety of computational techniques.<sup>7–10</sup> Most recently, density functional theory (DFT)-based Car–Parrinello (CP) molecular dynamics (MD)<sup>11</sup> have been successfully employed to study the liquid at ambient<sup>8,10</sup> and supercritical conditions.<sup>9</sup> We extend these studies and include quantum corrections to equilibrium properties arising from the nuclear degrees of freedom via path-integral (PI) simulations,<sup>12,13</sup> which have been demonstrated to reliably include quantum corrections in a wide range of H-bonded systems.<sup>14</sup> In the ensuing discussion, we will refer to liquid HF studied with classical CPMD and PICPMD as *C*- and *Q*-systems, respectively.

In agreement with previous CPMD simulations,<sup>8–10</sup> liquid HF is characterized by bent H-bonded zigzag chains of different length, which are entangled with each other and occasionally branched. The description of the nuclear motion (classical or PI) does not seem to influence the length and the spatial arrangement of the chains: the H···F–H angle in *C* and *Q* is, respectively, 115° and 114° with an rms amplitude of about 35° in both systems.

Quantitative information about the liquid structure can be obtained from the analysis of the radial distribution functions,  $g(r)$ . The functions related to hydrogen bonding are  $g_{FF}$  and  $g_{HF}$ . The former has a pronounced peak at about 2.5 Å that corresponds to the F···F distance of two H-bonded molecules. As can be seen from Figure 1a, this distance in *Q* (2.49 Å) is shorter than that in *C* (2.52 Å). Surprisingly, the peak in *Q* is sharper, indicating a more pronounced localization of two H-bonded F atoms. This finding is counterintuitive because one is first led to suppose that nuclear quantum (zero point energy) effects in *Q* should result in a broadening of the F···F peak.

A rationale for this behavior can be found in the analysis of  $g_{HF}$  (Figure 1b). Here, the first peak, which corresponds to the intramolecular H···F distance, has the expected trend on going from *C* to *Q*. In fact, because of the quantum delocalization of the

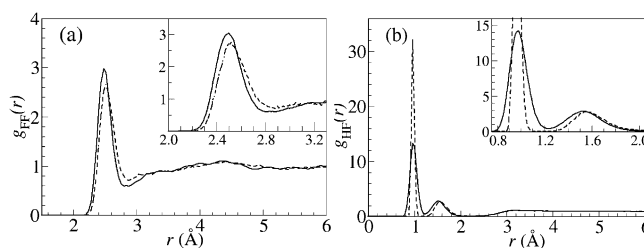


**Figure 1.** Radial distribution functions of liquid HF at 290 K: (a) F–F and (b) H–F. Dashed line, classical CPMD; solid line, PI-CPMD.

protons, the peak broadens and overlaps with the peak due to the H···F intermolecular H-bond. The average H–F bond length in *C* is 0.965 Å, which is 0.01 Å shorter than that in *Q*.<sup>16</sup> In *Q*, one also observes a shorter H-bond distance than in *C* (1.52 Å instead of 1.58 Å), due to an enhanced intermolecular interaction, which in turn leads to a reduction of the F···F nearest neighbor distance. Because of the quantum delocalization of the protons, the *Q*-system F–H proton gets closer to the F atom of a nearby molecule, enhancing the H-bonding and giving rise to a sharpening of the F···F peak.

The  $g_{HH}$  function (not shown) has the characteristic peak, which corresponds to the nearest neighbor intrachain H atoms. In *Q*, this peak appears at a shorter distance (2.14 Å) than in *C* (2.18 Å), an observation which also reflects the behavior just described above.

To characterize more quantitatively the shortening of the H-bond, we have investigated the wave functions obtained in the simulations. To this end, the center of charge of the maximally localized Wannier functions (WFC)<sup>17</sup> has been used to facilitate the interpretation of the electronic structure in terms of doubly occupied localized orbitals. This method has been shown to provide a vivid picture of the H-bond in liquid water.<sup>18</sup>

Unlike the formation of covalent bonds, which involves massive shifts of electron density, the rearrangement that occurs as a consequence of an H-bond is more subtle. Indeed, while the shifts of electron density that occur are relatively small, they are characteristic of H-bond formation: the larger the shift, the stronger the H-bond. Generally, there is an overall shift of electron density from the proton acceptor molecule to the donor. This density is drawn not only from the lone pair participating in the H-bond, but also from the entire molecule.<sup>19</sup>

In Figure 2, the position of the WFCs calculated for the monomer, dimer, and cyclic hexamer is reported along with the  $g(r)$  function of the pair F atom–WFC computed in the liquid phase. From the WFCs calculated for the clusters in vacuo, the above-mentioned density shift is clearly visible. In fact, as can be seen, the  $\sigma$  bond WFC gets closer to the F atom on passing from the monomer to the hexamer, whereas the WFC of the acceptor fluorine lone pair moves further away. This corresponds to a net shift of density toward the donor molecule. The cyclic hexamer, where each molecule donates and receives one H-bond, approaches the situation observed in the liquid phase.

<sup>†</sup> International School for Advanced Studies.

<sup>‡</sup> University of Pennsylvania.

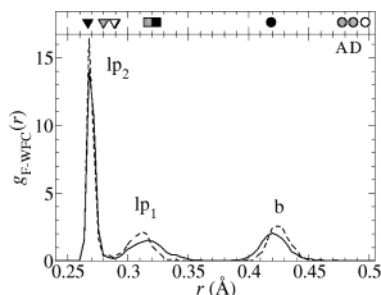


**Figure 2.** Radial distribution functions of the F atom–WFC pairs computed at 290 K from 15 configurations equally spaced in time. Dashed line, classical CPMD; solid line, PI-CPMD. The position of the WFCs with respect to the F atom calculated in vacuo for the monomer (empty symbols), dimer (gray-filled symbols), and cyclic hexamer (black-filled symbols) is also shown. Circles, squares, and triangles indicate covalent bond orbitals (b), H-bond acceptor lone pair ( $lp_1$ ), and nonbonded lone pair ( $lp_2$ ), respectively. A and D stand for acceptor and donor, respectively.

In liquid HF, because of the thermal fluctuations, there is a quite broad distribution of WFC positions. However, three distinct peaks are visible, which correspond to covalent bond orbitals, H-bond acceptor lone pairs, and nonbonded lone pairs, respectively. The magnitude of the electron density shift is larger in the *Q*- than in the *C*-system. In turn, this corresponds to a stronger H-bond. We observe in passing that the nonbonded lone pairs' distribution does not depend on the description of the nuclei.

The observed density shift going progressively from the gas phase to the condensed phase produces a larger and larger separation between the WFCs and the positive charged hydrogen nucleus and, therefore, leads to an increase of the net molecular dipole moment.<sup>17,18</sup> The computed monomer dipole moment is 1.82 D, which is in fairly good agreement with the experimental value of 1.91 D.<sup>20</sup> The dipole moment drastically increases from the monomer to the liquid. This parallels the trend of water dipole moment as calculated via DFT/BLYP-based ab initio MD.<sup>18a,b</sup> The average dipole moment in the *C* and *Q* simulations is 2.75 and 2.95 D, respectively. Thus, in *Q* there are stronger electrostatic and polarization interactions, which contribute to the shortening of the F...F intrachain distance. In these chains, the lone pairs are topologically distinct, so the orientation of the dipole moment does not coincide with the molecular axis. The average angle between the dipole moment and the F–H direction is 11° in both simulations, with an rms dispersion of 5°.

Surprisingly, the results presented in this Communication indicate a shorter H-bond in liquid HF when the nuclei are treated as quantum particles. Unfortunately, there are no experimental radial distribution functions of HF with which to compare our calculations. To date, experimental structural data have only been reported for DF. In this regard, our calculated differences between *C* and *Q* are comparable to the current experimental resolution of the structure factor determined for DF.<sup>4,5,21</sup> We are aware that our calculations could be affected by several errors. However, we can be confident that the approximations made do not change the qualitative picture given herein.<sup>22</sup>

In conclusion, our findings open important questions regarding the role of nuclear quantum effects on the structure of hydrogen-bonded systems. The present results suggest that in the case of strongly H-bonded liquids nuclear quantum effects can lead to stronger H-bonds. Taken at face value, this effect is likely to be present in biological systems, including proteins, enzymes, DNA, and RNA, where strong H-bonds are involved.<sup>1</sup> More calculations and experiments are deemed necessary to clarify this issue.

**Acknowledgment.** The work was supported by the National Science Foundation and a generous allocation of time on the tera-scale machine at the Pittsburgh Supercomputing Center.

## References

- (1) (a) Vock, P.; Engst, S.; Eder, M.; Ghisla, S. *Biochemistry* **1998**, *37*, 1848. (b) Northrop, D. B. *Acc. Chem. Res.* **2001**, *34*, 790.
- (2)  $T_b = 292.7$  K at 1 atm. Streng, A. G. *J. Chem. Eng. Data* **1971**, *16*, 357.
- (3) (a) Atoji, M.; Lipscomb, W. N. *Acta Crystallogr.* **1954**, *7*, 173. (b) Johnson, M. W.; Sandor, E.; Arzi, E. *Acta Crystallogr., Sect. B* **1975**, *31*, 1998.
- (4) Deraman, D.; Dore, J. C.; Powles, J. G.; Holloway, J. H.; Chieux, P. *Mol. Phys.* **1985**, *55*, 1351.
- (5) Pfeleiderer, T.; Waldner, I.; Bertagnolli, H.; Tödheide, K.; Fischer, H. *J. Chem. Phys.* **2000**, *113*, 3690.
- (6) (a) Janzen, J.; Bartell, L. S. *J. Chem. Phys.* **1969**, *50*, 3611. (b) Huisken, F.; Kaloudis, M.; Kulcke, A.; Laush, C.; Lisy, J. M. *J. Chem. Phys.* **1995**, *103*, 5366. (c) Quack, M.; Stohner, J.; Suhm, M. A. *J. Mol. Struct.* **2001**, *599*, 381.
- (7) For an overview of recent works employing empirical potential energy surfaces, see: (a) della Valle, R. G.; Gazzillo, D. *Phys. Rev. B* **1999**, *59*, 13699. (b) Jedlovsky, P.; Mezei, M.; Vallauri, R. *J. Chem. Phys.* **2001**, *115*, 9883 and references therein.
- (8) Roethlisberger, U.; Parrinello, M. *J. Chem. Phys.* **1997**, *106*, 4658.
- (9) Kreitmeir, M.; Bertagnolli, H.; Mortensen, J. J.; Parrinello, M. *J. Chem. Phys.* **2003**, *118*, 3639.
- (10) Kim, D.; Klein, M. L. *J. Am. Chem. Soc.* **1999**, *121*, 11251.
- (11) Car, R.; Parrinello, M. *Phys. Rev. Lett.* **1985**, *55*, 2471.
- (12) Marx, D.; Tuckerman, M. E.; Marthyna, G. J. *Comput. Phys. Commun.* **1999**, *118*, 166.
- (13) In the present DFT calculations, we have utilized Troullier–Martins pseudopotentials [Troullier, N.; Martins, J. L. *Phys. Rev. B* **1991**, *43*, 1993] to describe the atomic core of F atoms and a von Barth–Car pseudopotential [see, e.g., ref 15] for hydrogens. The valence wave functions have been expanded in plane-waves up to an energy cutoff of 70 Ry. We have employed the Becke, Lee, Parr, and Yang exchange and correlation functional (BLYP) [Becke, A. D. *Phys. Rev. A* **1988**, *38*, 3098. Lee, C.; Yang, W.; Parr, R. G. *Phys. Rev. B* **1988**, *37*, 785], which yield excellent results for both water<sup>15</sup> and HF.<sup>8,9</sup> The simulation cell consists of 54 HF molecules enclosed in a cubic box at the experimental density [Honda, K.; Kitaura, K.; Nishimoto, K. *Bull. Chem. Soc. Jpn.* **1992**, *65*, 3122]. The starting configuration for the simulations has been taken from previous studies.<sup>10</sup> The PI has been represented by 16 discrete beads. The equations of motion have been integrated with a time step of 0.121 fs using 800 au as a fictitious electronic mass.<sup>11</sup> The systems have been equilibrated at 290 K for 3 ps, and then the trajectories were collected for about 9 ps. To guarantee adiabaticity of the PI simulation, thermostats have been also applied to electrons.<sup>12</sup> All of the calculations have been performed by using the CPMD code [Hutter, J.; et al. CPMD (IBM Zurich Research Laboratory and MPI für Festkörperforschung, 2002)].
- (14) (a) Tuckerman, M. E.; Marx, D.; Klein, M. L.; Parrinello, M. *Science* **1997**, *275*, 817. (b) Benoit, M.; Marx, D.; Parrinello, M. *Nature* **1998**, *392*, 258. (c) Marx, D.; Tuckerman, M. E.; Hutter, J.; Parrinello, M. *Nature* **1999**, *397*, 601. (d) Tuckerman, M. E.; Marx, D. *Phys. Rev. Lett.* **2001**, *86*, 4946. (e) Tuckerman, M. E.; Marx, D.; Parrinello, M. *Nature* **2002**, *417*, 925.
- (15) Sprik, M.; Hutter, J.; Parrinello, M. *J. Chem. Phys.* **1996**, *105*, 1142.
- (16) These values should be compared to the value 0.932 Å computed at the same level of theory for the monomer in vacuo. The experimental value is 0.917 Å [Mason, M. G.; von Holle, W. G.; Robinson, D. W. *J. Chem. Phys.* **1971**, *54*, 3491].
- (17) Silvestrelli, P. L.; Marzari, N.; Vanderbilt, D.; Parrinello, M. *Solid State Commun.* **1998**, *107*, 7.
- (18) (a) Silvestrelli, P. L.; Parrinello, M. *Phys. Rev. Lett.* **1999**, *82*, 3308. (b) Silvestrelli, P. L.; Parrinello, M. *J. Chem. Phys.* **1990**, *111*, 3572. (c) Boero, M.; Terakura, K.; Ikeshoji, T.; Liew, C. C.; Parrinello, M. *Phys. Rev. Lett.* **2000**, *85*, 3245.
- (19) Scheiner, S. *Hydrogen Bonding: A Theoretical Perspective*; Oxford University Press: New York, 1997.
- (20) Hannay, N.; Smith, C. J. *J. Am. Chem. Soc.* **1946**, *68*, 171.
- (21) It is also worth observing that the F...F intrachain distance computed in both *C* and *Q* compares well with the distance measured for liquid DF at 293 K (2.56 Å)<sup>4</sup> and 300 K (2.53 Å),<sup>5</sup> and crystalline DF at 85 K (2.49 Å).<sup>3b</sup>
- (22) The largest source of error is likely the intrinsic error due to the use of the BLYP functional. Although DFT/BLYP calculations give good structural properties of H-bonded systems, it is not clear if polarization effects are equally well reproduced. However, any error should have the same influence in both *C* and *Q* simulations. Another error could be due to the small size of the simulation cell. Here, we have checked the influence of system size by performing simulations on a smaller simulation cell (27 molecules) with a smaller number of beads (8) to represent the PI. The overall picture is the same as the one discussed herein. Thus, the PI calculations are likely sufficiently well converged with regard to the (short-range) hydrogen-bonding patterns. We have also checked for size effects on the computed dipole moment without observing any relevant dependence (the average dipole moment difference between cells composed by 27 and 54 molecules is 0.04 D). Furthermore, the average net dipole moment of the entire cell is negligible (about 0.2 D) in all cases. Hence, we can rule out strong dipole–dipole interactions between the cell and its images.

JA0351995